

Capillary filling in patterned channels

H. Kusumaatmaja,¹ C. M. Pooley,¹ S. Girardo,² D. Pisignano,² and J. M. Yeomans¹

¹Rudolf Peierls Centre for Theoretical Physics, 1 Keble Road, Oxford OX1 3NP, United Kingdom

²NNL, National Nanotechnology Laboratory of Istituto Nazionale di Fisica della Materia-CNR and Scuola Superiore ISUFI, Università del Salento, via Arnesano, I-73100 Lecce, Italy

(Received 12 February 2008; published 17 June 2008)

We show how the capillary filling of microchannels is affected by posts or ridges on the sides of the channels. Ridges perpendicular to the flow direction introduce contact line pinning, which slows, or sometimes prevents, filling, whereas ridges parallel to the flow provide extra surface that may enhance filling. Patterning the microchannel surface with square posts has little effect on the ability of a channel to fill for equilibrium contact angle $\theta_e \leq 30^\circ$. For $\theta_e \geq 60^\circ$, however, even a small number of posts can pin the advancing liquid front.

DOI: 10.1103/PhysRevE.77.067301

PACS number(s): 47.61.-k, 47.55.nb, 68.08.Bc

Recent years have seen rapid progress in the technology of fabricating channels at micrometer length scales. Such microfluidic systems are increasingly finding applications, for example, in diagnostic testing and DNA manipulation and as microreactors. As narrower channels are used to conserve space and reagents, surface effects will have an increasing influence on the fluid flow. In particular, it may be possible to exploit the chemical or geometrical patterning of a surface to control the flow within the channels. Indeed, first steps in this direction have already been taken: for example, Joseph *et al.* used superhydrophobic surfaces to introduce slip lengths of the order of a few μm [1], Zhao *et al.* used hydrophilic stripes to confine fluid flows [2], and Stroock *et al.* used oriented grooves to enhance mixing [3].

In this Brief Report, we describe the way in which a fluid penetrates a microchannel patterned with posts or ridges. We find that the hysteretic behavior that results from the surface patterning can be a substantial factor in controlling how the fluid moves down the channel. Ridges or posts oriented parallel to the flow speed up capillary filling while those perpendicular to the flow pin the interface and suppress, or sometimes prevent, filling. We investigate the rate at which the microchannel fills, finding that it is highly dependent on both the geometry and the spacing of the posts. In particular, we demonstrate that a patterned surface can act as a valve, allowing filling in one direction only.

The classical analysis of capillary penetration is due to Washburn [4]. Consider a capillary of width h with an infinite reservoir of liquid of dynamic viscosity η at one end. If the walls of the capillary are hydrophilic, the liquid will move to fill it with a mean velocity (assuming two-dimensional Poiseuille flow), $\bar{v} = -\frac{h^2}{12\eta} \frac{dp}{dx}$, where $\frac{dp}{dx}$ is the pressure gradient that sets up the flow. The driving force for the flow is provided by the decrease in free energy as the fluid wets the walls or, equivalently, the Laplace pressure across the interface. Hence $\frac{dp}{dx} = -\frac{\gamma}{Rl}$, where γ is the surface tension of the liquid interface, $R = h/2 \cos \theta_a$ is its radius of curvature, and l is the length of liquid in the tube. Substituting $\frac{dp}{dx}$ into the parabolic flow profile and using $\bar{v} = dl/dt$ gives Washburn's law $l = (\gamma h \cos \theta_a / 3 \eta)^{1/2} (t + t_0)^{1/2}$, where t_0 is an integration constant. Note that it is appropriate to use not the static but the advancing contact angle θ_a , as this controls the curvature of the interface and hence the Laplace

pressure. Washburn's law assumes that there is no resistance to motion from any fluid already in the capillary. The derivation also assumes incompressibility, and neglects inertial effects [6,7], gravity [8], and any deviations from a Poiseuille flow profile at the inlet or the interface [7,9–11].

Our aim is to explore capillary filling in the presence of topological patterning on the surface of the capillary. Simple arguments, based on Gibbs' criterion [5], will suffice to explain when capillary filling is not possible for one-dimensional surface patterning (ridges). However, to see how the rate of filling is affected by the surface relief, and to consider two-dimensional surface topologies, we will need to solve the hydrodynamic equations of motion of the fluids. Therefore, we first describe the numerical model we shall use, a diffuse interface representation of a binary fluid, and check that it reproduces Washburn's law for simple capillary filling.

We consider an immiscible binary fluid, comprising components A and B say, described, in equilibrium, by the Landau free energy

$$\int_V dV \left(\frac{\alpha}{2} \phi^2 + \frac{\beta}{4} \phi^4 + \frac{\kappa}{2} (\nabla \phi)^2 + T \rho \ln \rho \right) - \int_S dS (\sigma \phi), \quad (1)$$

where $\rho = \rho_A + \rho_B$ is the total fluid density and $\phi = \rho_A - \rho_B$ is the concentration. We chose $\alpha = -\beta$ so that the two possible bulk concentrations are $\phi = 1.0$ and -1.0 . κ is related to the surface tension by $\gamma = \sqrt{8\kappa\beta/9}$ and T is chosen to be $1/3$ to minimize the error terms. The surface contribution allows us to tune the equilibrium contact angle by varying σ [12].

The fluid motion is described by the continuity, Navier-Stokes, and convection-diffusion equations,

$$\partial_t \rho + \partial_\beta (\rho u_\beta) = 0, \quad (2)$$

$$\partial_t \rho u_\alpha + \partial_\beta (\rho u_\alpha u_\beta) = -\partial_\beta P_{\alpha\beta} + \partial_\beta S_{\alpha\beta}, \quad (3)$$

$$\partial_t \phi + \partial_\beta (\phi u_\beta) = M \partial_\beta^2 \mu, \quad (4)$$

where \vec{u} is the fluid velocity, $P_{\alpha\beta}$ and $S_{\alpha\beta}$ are the pressure and stress tensors, respectively, μ is the chemical potential, and M is a mobility. We solve these equations using a lattice Boltzmann algorithm, described in detail in [12]. Similar

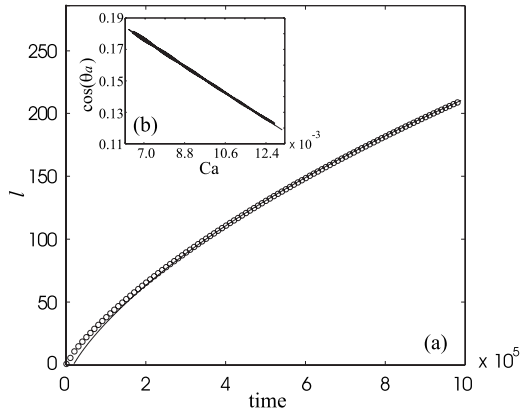


FIG. 1. Lattice Boltzmann simulation results for capillary filling for $h=50$, $\theta_e=60^\circ$, $\gamma=0.0188$, $\rho_A=\rho_B=1.0$, $\eta_A=0.83$, $\eta_B=0.03$, and $M=0.05$. (a) The length of the column of the filling A component plotted against time. The circles are the simulation results and the solid line is a fit to Washburn's law using the measured advancing contact angle and correcting for the small viscosity of the displaced B component. (b) The measured advancing contact angle of the liquid-liquid interface: note that $\cos \theta_a$ varies linearly with capillary number [13].

models have also been recently used in [7,8] to simulate capillary filling on smooth surfaces.

Numerical results showing capillary filling of a smooth channel are presented in Fig. 1(a). The plot is for a channel of length $L=640$, infinite width, and height $h=50$. Reservoirs (480×200) of components A and B are attached at each end of the capillary. The two reservoirs are connected to ensure that they have the same pressure. The parameters of the model (given in the caption of Fig. 1) are chosen so that the

capillary and Reynolds numbers are of order 10^{-2} .

The solid line in Fig. 1(a) is a fit to Washburn's law using the measured values of the contact angle and correcting for the small viscosity of the displaced B component. The fit is excellent, except very close to the beginning of the simulation where the expected deviations from Washburn's law due to inertial effects and deviations from a Poiseuille flow profile are observed. Figure 1(b) shows the measured $\cos \theta_a$, which decreases linearly as the capillary number decreases [13].

We now discuss capillary filling in a channel with topological patterning on the surface. On stepped surfaces, the driving force of the Laplace pressure must be sufficient to overcome any hysteresis due to the surface patterning. We shall assume that the contact angle of the A component is $<90^\circ$, i.e., this is the fluid that may fill the capillary, and that there is no intrinsic hysteresis.

We first consider two dimensions, and a channel where one of the walls is patterned by square posts, as shown in Fig. 2(a). (The same results apply for a three-dimensional channel with ridges that are translationally invariant perpendicular to the flow.) According to Gibbs' criterion, for an interface moving very slowly, the contact line will remain pinned on the edge of the posts until θ_p , the angle the interface makes with the side of the posts, reaches the equilibrium contact angle θ_e . It follows immediately [see Fig. 2(a)] that there will be no capillary filling unless

$$\theta_p \equiv 90^\circ - \theta_e < \theta_e, \tag{5}$$

that is, $\theta_e < 45^\circ$. If the surface is patterned by triangular posts, with sides at an angle α to the edges of the channel as shown in Fig. 2(b), the condition for capillarity is less strin-

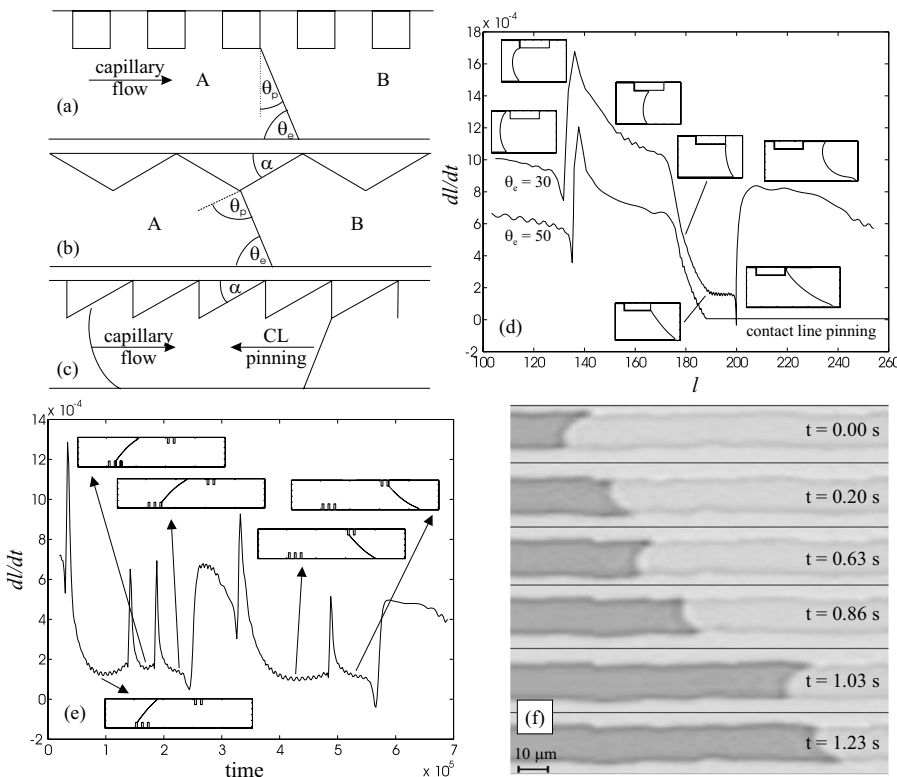


FIG. 2. Pinning of the contact line during capillary filling when the top wall is patterned with (a) squares, (b) triangles, and (c) ratchets. (d) Interface velocity dl/dt when one of the walls is decorated with a single 40×10 post. (e) Interface velocity when the bottom wall is decorated with three posts and the top wall is decorated with two posts. The posts have height 10 and width 5. (f) Experimental results on capillary filling in patterned channels. Local pinning temporarily holds the capillary front on one of the two microchannel sidewalls, while the interface advances along the opposite sidewall.

gent, namely $\theta_e < 90^\circ - \alpha/2$. Hence the surface in Fig. 2(c) will allow filling from left to right, but not from right to left if $45^\circ < \theta_e < 90^\circ - \alpha/2$.

Numerical results showing how the interface behaves as it approaches a post with finite velocity are presented in Fig. 2(d) for channel height $h=50$, post height $h_p=10$, post width $w_p=40$, and equilibrium contact angles $\theta_e=30^\circ$ and 50° . Here l , the length of the liquid column, is measured at the center of the capillary channel. As the interface approaches the post, it is slowed down by dissipation caused by the post. However, once the interface is able to respond to the wetting potential of the post, it quickly wets the leading edge. The interface slows as it moves over the top of the post—if the post were infinite in extent, it would reach the speed appropriate to a channel of height $h-h_p$. Once the trailing edge of the post is reached, there is a substantial decrease in velocity as the interface becomes pinned. For $\theta_e=30^\circ$, the interface is able to proceed, but for $\theta_e=50^\circ$ it remains pinned, consistent with the condition in Eq. (5). For the same value of θ_e , the variation in velocity is more pronounced for higher posts.

Figure 2(e) shows the dynamics as the interface moves along a capillary with groups of posts on both the top and bottom surfaces of the channel. This simulation demonstrates several features of the motion. First, as the interface reaches the three posts on the lower edge of the channel, it takes longer to depin from the first post it reaches. This is because the free end of the interface takes time to slide along the top of the capillary until it reaches an angle where it can pull the pinned end away from the trailing edge of the post. For the second and third posts, the interface is already aligned diagonally across the channel and does not need to move so far. Once the interface reaches the posts at the top of the channel, it remains pinned on the first of these for some time until the interface again takes up a diagonal configuration, but now with the bottom edge leading.

Such switching between two diagonally aligned interface configurations has been observed in experiments on capillary filling in channels with lateral root-mean-square roughness $1 \mu\text{m}$, as shown in Fig. 2(f). The channels were realized by optical lithography employing plastic photomasks patterned with a laser printer. Polymer microchannels were then obtained by subsequent replica molding with polydimethylsiloxane. A $2 \mu\text{l}$ drop of water was released at the entrance of the microchannels and the penetrating interface was imaged by a 320×240 pixels, 30 fps camera. Experiments have also shown the interface waiting longer at the beginning of a line of posts engineered to lie on one surface of a microchannel.

We now consider two-dimensional surface patterning. Both walls of the capillary are patterned with 20×20 square posts of height 10. The posts face each other across the channel, which is of height $h=50$. They are separated by spaces of length D in the direction perpendicular to the flow. This geometry is illustrated in Fig. 3(a), which shows a side view of the channel. For $D=0$, the case corresponding to ridges across the channel, Gibbs' criterion predicts that the interface will always remain pinned between the trailing edges of a pair of opposing posts. For $D \neq 0$, however, the motion can be driven by the portion of the interface that lies between the posts.

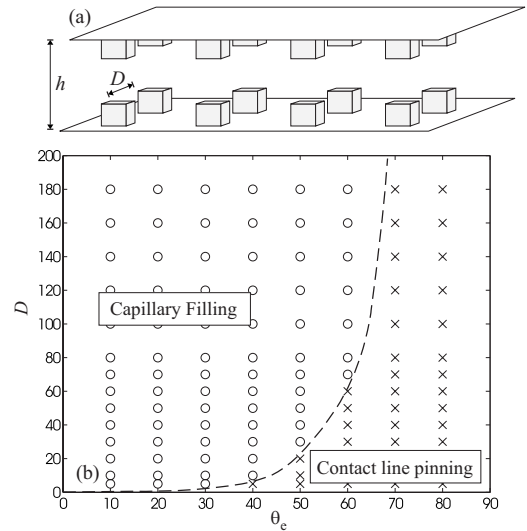


FIG. 3. Two-dimensional surface patterning: (a) the surface geometry; (b) regions of contact line pinning and capillary flow as a function of post-separation and equilibrium contact angle. The channel height is kept constant at $h=50$. The dashed line is a guide to the eye.

Figure 3(b) shows the crossover between capillary filling and contact line pinning as a function of D and θ_e . For $\theta_e \leq 30^\circ$, a small gap in between the posts is enough to allow filling. As the interface moves through the gap and protrudes beyond the posts, it is able to depin, initially from the side of the posts.

For $\theta_e \geq 60^\circ$, however, filling is strongly suppressed. This is due to two complementary effects: the force driving the interface through the gaps becomes weaker and the pinning on the sides of the posts becomes stronger. Note that the part of the interface that lies in between the posts can bow out further as D is increased and it is possible that the leading interface could touch the next row of posts, thus providing an alternative mechanism to depin the interface from the edges of the posts.

We have also varied the relative height of the posts with respect to the channel width and find that the contact line pinning condition depends only very weakly on the channel height. This is because the interface behavior is primarily determined by depinning from the side edges of the posts. It is also worth noting that we neglect fluctuations in our simulations.

So far, we have considered surfaces patterned with ridges oriented perpendicular to the flow and square posts, cases in which pinning by the posts suppresses, or even prevents, capillary filling. We now identify a situation in which patterning can be used to speed up capillary flow, with ridges aligned *along* the flow direction. In Fig. 4, we compare the lengths of the A column, plotted as a function of time, for a channel of height $h=50$ with infinitely long ridges of width (w_p), height (h_p), and separation (D) (i) 5, 5, and 10; (ii) 8, 5, and 7; and (iii) 10, 10, and 20 lying along the channel. In all these cases, the channels have the same surface roughness $r=1+2h_p/(w_p+D)=5/3$. For comparison, we also show smooth channel simulations for $h=40$ and 50. It is clear from Fig. 4 that it is possible to increase the rate of capillary filling

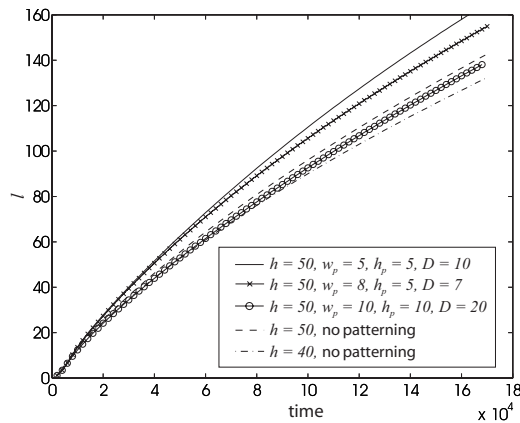


FIG. 4. The length of the column of A liquid plotted against time for different surface patterning. The channels' intrinsic contact angle is $\theta_e = 30^\circ$. Other parameters as in Fig. 1.

by patterning the channels [cases (i) and (ii)]. This occurs because there is no contact angle hysteresis in this geometry and because the total surface area per unit length wetted by the A liquid is increased over the flat channel value by the roughness factor r . However, from Fig. 4 it is apparent that the rate of filling is not just controlled by r . This is because surface roughness distorts the liquid flow from a parabolic profile and hence increases the dissipation. As shown in Fig. 4, the dissipation increases as the distance between two neighboring ridges is reduced [case (ii)] and as the size of the

ridges relative to the channel height is increased [case (iii)]. The filling speed is a competition between the increased energy gain of wetting a grooved channel and the additional dissipation caused by the distortion of the flow.

Our results suggest strategies that could be used to design surface patterning on microfluidics channels. To speed up capillary filling, one should introduce roughness that is elongated in the direction of the flow. However, additional surface area will only speed up filling if pinning is avoided by, for example, avoiding sharp edges and making the post-inclinations as gentle as possible. Furthermore, any surface patterning should neither be too dense nor too large to minimize dissipation. Random arrangement of the posts may also be used to avoid the cooperative interface pinning effect. Finally, the intrinsic contact angle of the materials is $\theta_e \approx 60^\circ$ for capillary filling down a rough channel. These results are consistent with recent findings by Kohonen [14], who found that the walls of the tracheids in the dry-habitat species are typically rougher than those in the wet-habitat species, and with $\theta_e \sim 40^\circ$. Moreover, the set of design principles we describe above may help explain why certain types of wall sculpturing, such as helical thickening [15] found on tree capillaries, are more common than others.

We thank L. Biferale and S. Succi for useful discussions. H. K. acknowledges support from a Clarendon Fund (Oxford University Press) and the INFLUS project.

-
- [1] P. Joseph *et al.*, Phys. Rev. Lett. **97**, 156104 (2006).
 [2] B. Zhao *et al.*, Science **291**, 1023 (2001).
 [3] A. D. Stroock *et al.*, Science **295**, 647 (2002).
 [4] E. W. Washburn, Phys. Rev. **17**, 273 (1921).
 [5] J. W. Gibbs, *Scientific Papers 1906* (Dover, New York, 1961) (Dover reprint).
 [6] D. Quéré, Europhys. Lett. **39**, 533 (1997).
 [7] F. Diotallevi *et al.*, arXiv:0707.0945.
 [8] P. Raiskinmäki *et al.*, J. Stat. Phys. **107**, 143 (2002).
 [9] S. Levine *et al.*, J. Colloid Interface Sci. **73**, 136 (1980).
 [10] J. Szekeley, A. W. Neumann, and Y. K. Chuang, J. Colloid Interface Sci. **69**, 486 (1979).
 [11] D. I. Dimitrov, A. Milchev, and K. Binder, Phys. Rev. Lett. **99**, 054501 (2007).
 [12] A. J. Briant and J. M. Yeomans, Phys. Rev. E **69**, 031603 (2004).
 [13] M. Latva-Kokko and D. H. Rothman, Phys. Rev. Lett. **98**, 254503 (2007).
 [14] M. M. Kohonen, Langmuir **22**, 3148 (2006).
 [15] A. A. Jeje and M. H. Zimmermann, J. Exp. Bot. **30**, 817 (1979).